

## VI. TUBE RESEARCH AND DEVELOPMENT

### A. MAGNETRON DEVELOPMENT

Prof. S. T. Martin	J. G. Lawton
A. G. Barrett	R. R. Moats
D. L. Eckhardt	R. J. Renfrow

#### 1. High-Power 10.7-Cm Magnetron

##### a. Testing and design

To facilitate the construction of the high-power magnetron, the entire output section, including the quarter wave transformer and window, has been redesigned. The new design is based on standard S band waveguide. The quarter wave transformer was changed to increase the external loading of the tube. Cold test measurements on a tube with the redesigned output section give an external Q of 230.

Work is in progress to build and test eight or more magnetrons. It is expected that all of these tubes will have ceramic cathode leads and that at least four of them will have thoria cathodes. The change to ceramic cathode leads will necessitate some slight redesign of the anode, and the change to the thoria cathode will require lengthening of the end spaces and further cold testing to detect and then eliminate possible spurious end space resonances.

##### b. Thoria cathodes

Considerable difficulty has been experienced in obtaining a large molybdenum-thoria cathode for use in the magnetron. Trial cathodes pressed in the split segment die were not of sufficient length or diameter after sintering, and an excessive amount of hour-glassing was evident in the sintered cathodes. The difficulty was traced to the extremely fine particle size of the thoria powder used in the compacting process, and after considerable experimentation a suitable particle size has been chosen and the problem solved.

The mathematical investigation of the heat-conducting and dissipation properties of the end mounts for the thoria cathode has been completed with use of the electronic differential analyzer. The results show that if the thickness of the sheet tantalum or molybdenum used in the end mounts is 0.007 in. or greater, there should be no difficulty from failure of the end mounts at high temperatures.

The experiment on platinum-brazing the tantalum end mounts to the thoria cathode in a helium atmosphere has been successfully completed. A small thoria cathode and end mount together with the platinum solder were supported on a molybdenum spider inside a Vicor tube. A tantalum cylinder around the cathode provided the heating element. Pure helium was introduced through a fitting at the bottom of the Vicor tube and permitted to flush for 20 minutes to insure an inert atmosphere. At the end of that time power was

## (VI. TUBE RESEARCH AND DEVELOPMENT)

slowly applied to the tantalum cylinder by r-f induction. A moderate flow of helium was maintained while the temperature of the tantalum cylinder was brought to 1800°C; at this temperature the platinum solder flowed. The power was then shut off while the helium continued to flow for 40 minutes as the cathode cooled. After another 20 minutes the cathode had cooled to room temperature and was removed. No discoloration of the tantalum was observed, and a satisfactory braze had been effected between the end mount and the cathode.

### c. 20-megawatt modulator

A previous Progress Report mentioned the difficulties encountered with the 20-Mw spark-gap modulator. More recently, r-f bridge measurements have been made on the 20-ohm pulse cable, and pulse measurements have been made on the pulse-forming networks. A fundamental error in design calculations of the pulse-forming networks has been found. A new inductor for the 1- $\mu$ sec pulse-forming network has been designed and will shortly be constructed.

## 2. Magnetron Research

### a. Mode interaction in magnetrons

A cold test of the  $n = 3$  resonance of a 718EY magnetron in the  $\pi$ -mode ( $n = 4$ ) has been carried out using techniques described in the last Quarterly Progress Report. These results show increasing loading of the  $n = 3$  mode as amplitude of  $\pi$ -mode oscillation increases and anode current and voltage increase correspondingly. It is also observed that when there is preoscillation anode current flowing, the electron stream loads the  $n = 3$  mode. A plot of standing wave ratio as a function of wavelength of the injected signal for several conditions of operation is shown in Fig. VI-1.

A series of tests is now under way to determine the effect of changing the output coupling of the 718EY upon the phenomena described above.

### b. Noise properties of the preoscillating magnetron

Further work on this subject has been postponed pending completion of the problem of manufacturing and mounting thoria cathodes for the high-power magnetron.

### c. Mode identification in magnetrons

While the anode used in the high-power magnetron is designed to operate in the  $\pi$ -mode,  $n = 9$ , at 2800 Mc/sec ( $n$  is the number of times the r-f pattern repeats itself around the periphery of the anode), oscillation in other modes is possible. If the resonant frequencies corresponding to the various modes of resonance are determined, the starting voltages of all modes of operation as a function of magnetic field can be

(VI. TUBE RESEARCH AND DEVELOPMENT)

determined by means of Hartree's equation. These resonant frequencies have been calculated (1); the highest calculated frequency, corresponding to  $n = 5$ , is 3455 Mc/sec and the lowest calculated resonant frequency, corresponding to  $n = 1$ , is 1442 Mc/sec.

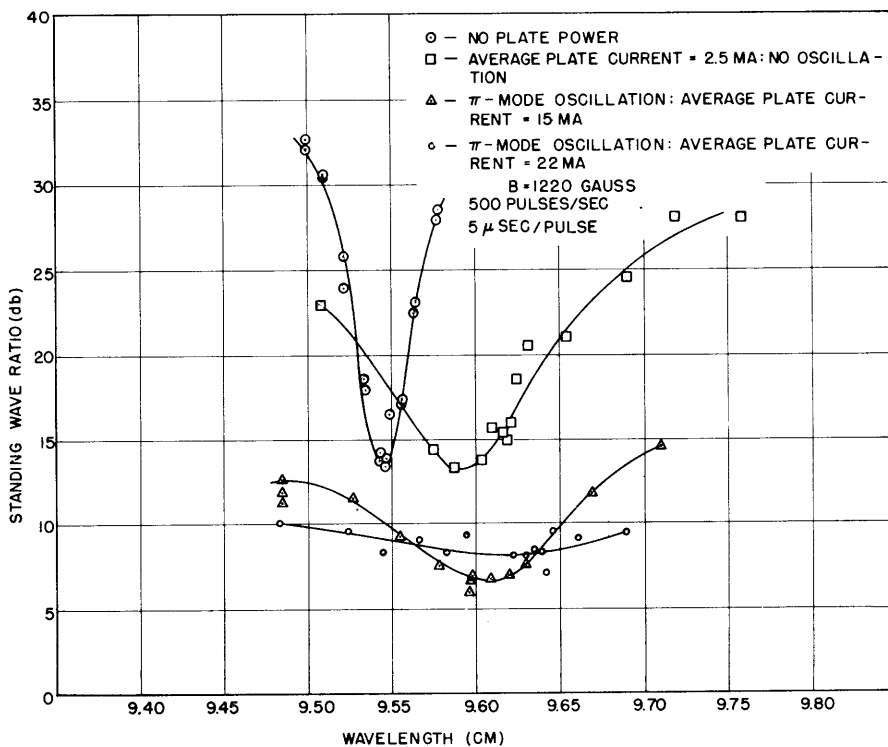


Fig. VI-1 Test of  $n = 3$  resonance in 718EY magnetron ( $\pi$ -mode:  $n = 4$ ).

In order to verify these calculations, a rotating probe is being constructed which will make possible the observation of the r-f field as a function of the angle of probe rotation. R-f energy is fed into the magnetron through its output section from a klystron oscillator. The signal picked up by the rotating probe is detected by means of a crystal, and fed through slip rings to an amplifier and then to the vertical deflection plates of a cathode ray oscillograph. The sweep is synchronized with the rotation of the probe. The resulting pattern is therefore a plot of the magnitude of the r-f signal versus angle of rotation. The mode of resonance is identified from this pattern (2).

In order to carry out these tests with available waveguides and klystron oscillators, some of the measurements will be made on a wavelength-scaled model of the original tube in which all the dimensions were reduced by a factor of 3.38.

References

- (1) The resonant frequencies were calculated with the aid of the curves appearing in Fig. 3.10, Radiation Laboratory Series, 6, 101.
- (2) For some aspects of mode identification from the oscillograph patterns, see Technical Report No. 99, Research Laboratory of Electronics, M. I. T.

## (VI. TUBE RESEARCH AND DEVELOPMENT)

### 3. Cathode Research

The peculiar emission characteristics of the experimental diode reported in the last Quarterly Progress Report can be explained on the basis of the behavior of an insulator used for supporting and centering the cathode. The tube construction is shown in Fig. VII-3, page 37, Quarterly Progress Report, October 15, 1949.

When the cathodes of the experimental tubes had been examined after processing and emission measurements, a dark deposit was observed on both the cathode coating and supporting insulator, while the nickel sleeve was still bright and shiny. A qualitative test for nickel in the darkened surface of the insulator gave a strong positive indication. The discoloration on both the insulator and cathode coating was nickel evaporated from the anode during the prolonged processing at high temperature.

This nickel coating acts as a resistance in parallel with the diode; the resistance is variable with temperature. Such a condition accounts for the temperature sensitivity of the cathode emission and the increase in emission above the calculated space-charge-limited emission. The nickel coating on the insulator will also disturb the axial symmetry of the electric field, thereby making invalid the basic assumption under which the Langmuir-Childs emission is calculated.

## B. MICROWAVE TUBES

L. D. Smullin

L. A. Harris

A. Karp

G. W. Zeoli

### 1. Microwave Noise Studies

Progress in studying the noise in an electron beam at 2840 Mc may be described under the following headings: completion of noise-measuring equipment; completion of two successful noise-study vacuum tubes; compilation of experimental data obtained with these tubes; development of a theory applicable to the case under study; completion of design and commencement of construction of a third vacuum tube.

#### a. Equipment for measuring noise at 2840 Mc

The noise output from the resonant cavity to which the noise in the beam is coupled is in a band about 4 Mc wide centered at 2840 Mc, and is measured by comparing it with the noise from a standard source. This standard source, comprising a desk-lamp fluorescent tube, as conceived by Mumford (1), was described in the Progress Report, October 15, 1949. Since then a significant change in the construction has been adopted. The lamp (a 12-in. G.E. F8T5) is now located obliquely across the waveguide so that, like a tapered strip of resistive material, it is matched over a very wide band, making a more useful laboratory instrument than the previous model.

(VI. TUBE RESEARCH AND DEVELOPMENT)

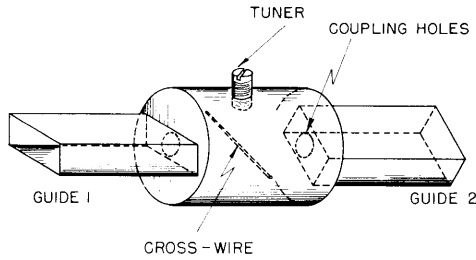


Fig. VI-2 Filter with variable loaded Q.

A filter is needed so that the standard and unknown noise signals may have the same bandwidths, which is necessary if a direct comparison is to be made. For this purpose a cylindrical resonant cavity was built as shown in Fig. VI-2. The cross-wire renders the cavity asymmetrical with respect to the axis of the cylinder so that as the waveguides are rotated with respect to this wire (special flanges were made to facilitate this) various degrees of coupling can be achieved at

each end. In this way the bandwidth and S.W.R. can be made equal to that of the cavity in the noise-study vacuum tube.

The microwave receiver remains as described in the October report except for a change in the method of introducing L.O. power into the mixer. A directional coupler is now used to minimize the amount of L.O. power incident on the noise sources.

A noise measurement is essentially as follows.

Notation:

$I$  = beam current

$e$  = electron charge

$\overline{i^2}$  = mean-square fluctuation current in beam in band  $\Delta f$

$\Gamma^2$  = number by which  $(2eI\Delta f)$  may be multiplied to give  $\overline{i^2}$   
(includes space-charge reduction factor)

$R$  = cavity resonant impedance at the gap

$S_o$  = V.S.W.R. of cavity at resonance

$\mu^2$  = beam coupling coefficient

$A$  = attenuator setting expressed as a ratio  
output power/input power

$a$  = transmission of filter cavity at resonance, expressed as a fraction  
output power/ input power

$k$  = Boltzmann's constant

$T_s$  = noise temperature of standard source

If  $A_s$  and  $A_x$  are the attenuator settings that give equal receiver outputs for the standard source and for the noise tube, respectively, then

$$\Gamma^2 = \frac{A_s a k T_s (1 + S_o)^2}{2A_x e I \mu^2 R S_o} \quad (1)$$

(VI. TUBE RESEARCH AND DEVELOPMENT)

R is measured by determining the rate of change of resonant wavelength with the insertion of a small metallic volume into the cavity (2), and  $\mu^2$  is computed from formulae derived in Reference 3. The main uncertainties in the noise measurements are in the evaluation of R and  $\mu^2$ .

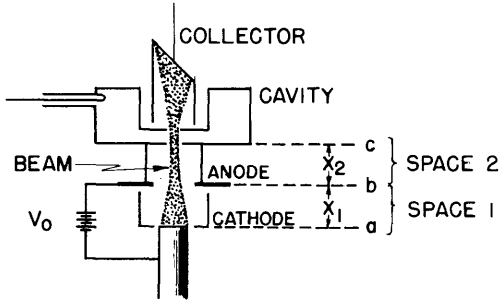


Fig. VI-3 Configuration of beam-noise tube.

b. A basic theory

The method of treatment which seems to have the greatest potentialities for analyzing our problem may be called the Llewellyn-Peterson Procedure (4,5). It consists of breaking up the various portions of the tube into parallel-plane diodes, using the end conditions of each stage as the initial conditions for the next. An outline of our analysis follows.

Notation: (see also Fig. VI-3 and the preceding notation)

$U_0$  = d-c beam velocity at full voltage,  $V_0$

$u$  = a-c component of velocity

$q$  = a-c component of convection current density

$i$  = a-c total current (density)

$v$  = a-c voltage across a diode section

$\tau$  = d-c transit time

$T_k$  = cathode temperature

$\eta$  = ratio of electron charge to mass

For space 1, the Llewellyn-Peterson linear equations are

$$v_{ab} = 0 = A_1^* i_1 + B_1^* q_a + C_1^* u_a \quad (2)$$

$$q_b = D_1^* i_1 + E_1^* q_a + F_1^* u_a \quad (3)$$

$$u_b = G_1^* i_1 + H_1^* q_a + I_1^* u_a \quad (4)$$

and a similar set applies for space 2. Because space 1 is a region of space-charge-limited flow (see the original references (4,5) where the coefficients denoted by starred letters are evaluated),  $E_1^* = B_1^* = H_1^* = 0$ , and we can solve our linear equations to get

(VI. TUBE RESEARCH AND DEVELOPMENT)

$$q_c = \left[ (E_2^* - D_2^* B_2^*/A_2^*)(F_1^* - C_1^* D_1^*/A_1^*) + (F_2^* - C_2^* D_2^*/A_2^*)(I_1^* - G_1^* C_1^*/A_1^*) \right] u_a \quad (5)$$

which expresses the convection current modulation  $q_c$ , which excites the cavity, in terms of the velocity modulation  $u_a$  at the virtual cathode. According to Rack's (7) analysis of noise in a space-charge-limited diode

$$\overline{u_a^2} = (4 - \pi)(\eta/I) kT \Delta f \quad (6)$$

Continuing to evaluate the coefficients  $A^*$ ,  $B^*$ , ..., according to Reference 5, we can finally obtain

$$\Gamma_{(\text{plane } c)}^2 = \frac{(4 - \pi) kT k \omega^2}{8 e \eta V_0^2} (U_0 \tau_1 - U_0 \tau_2)^2 \quad (7)$$

In space 2, because the beam is not very dense,  $U_0 \tau_2 = x_2$ . If space 1 were a plane-parallel, space-charge-limited diode we would have  $U_0 \tau_1 = 3x_1$ , but we must note that we actually have a Pierce-type electron gun where the flow is between concentric spheres instead of parallel planes. The transit time of a space-charge-limited, concentric-sphere diode has not been evaluated in any known literature, so we have had to solve this problem, whose results are expressible as  $U_0 \tau_1 = 3h x_1$ . The correction factor  $h$ , which turns out to be a universal function of the ratio of spherical radii, is shown in Fig. VI-4. (In our experimental gun  $h$  is about 1.5, and hence is important.)

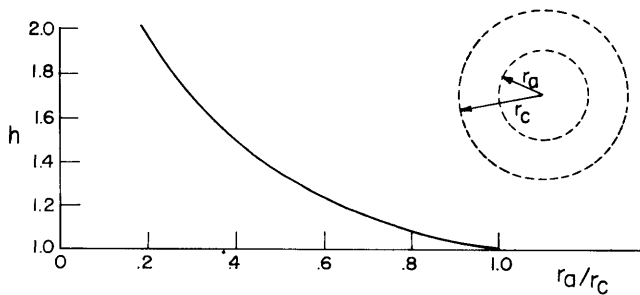


Fig. VI-4

Factor for computing transit time of a space-charge-limited, concentric-sphere diode, with initial velocities neglected.  $h$  = ratio of transit time of this diode to that of a space-charge-limited parallel-plane diode of same spacing.

A serious fault can be found in the foregoing analysis. The coefficients  $A_1^*$ ,  $B_1^*$ , ..., as evaluated in References 4 and 5, for space 1, involve in their computation the space-charge repulsion forces in the space-charge-limited region. The evaluations of these forces in the References are for flow between infinite, parallel planes, but in our Pierce gun we have a converging beam of small diameter, and it can be shown that the forces here are quite different from the case of infinite, parallel planes.

At present, partition effect can be treated theoretically only if we assume the condition known in the literature as superposed flow. This would require that the probability of an electron's striking the edge of the hole be independent of the point in the cathode

(VI. TUBE RESEARCH AND DEVELOPMENT)

whence the electron came. North (8) has worked out the theory for this case. Thus, if

$$p_c = \frac{\text{current intercepted}}{\text{current incident}} \quad \text{at plane } c$$

$$\Gamma^2 = \overline{i^2} / 2e I \Delta f \quad \text{when } p_c = 0$$

$$(\Gamma^2)' = i^2 / 2e I_{(\text{through})} \Delta f \quad \text{when } p_c \neq 0$$

then 
$$(\Gamma^2)' = \Gamma^2 + p_c(1 - \Gamma^2) \quad . \quad (8)$$

From this we see that if  $\Gamma^2$  is of the order of 0.05,  $p_c$  must be less than 0.01 if we are to assume  $\Gamma^2 \approx (\Gamma^2)'$ .

c. Experimental tubes

After three cases of cathode contamination and one envelope fracture, we finally completed two tubes containing a Pierce gun, a cavity, and a collector (Fig. VI-5). In one (No. I-4) the distance  $x_2$  was 1 1/8 in. and in the other (No. I-A-6),  $x_2$  was 1/2 in.

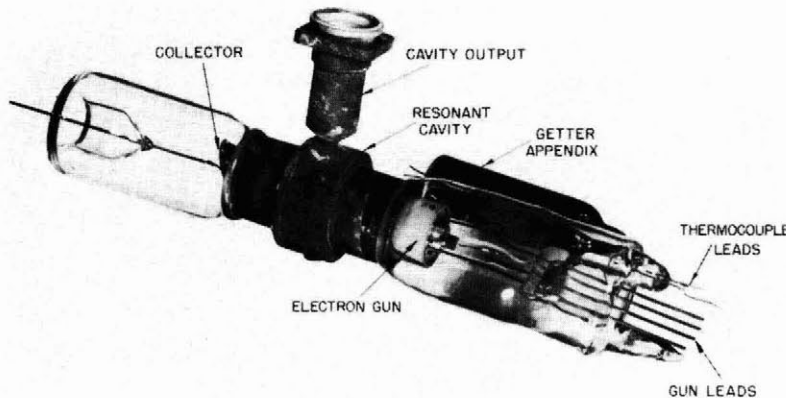


Fig. VI-5 Tube for measuring shot-noise in an electron beam at 2840 Mc.

In designing I-A, some preliminary tests on the gun were made to find experimentally the distance from the anode at which the beam has its minimum diameter, so that the cavity could be placed at this point to keep  $p_c$  as low as possible. For this purpose the beam-exploring techniques described elsewhere in this report were used. In tube I-A-6,  $p_c$  usually appeared to be less than 1 or 2 percent, but we believe the real value of  $p_c$  to be quite negligible because the stray current is intercepted not at plane c, but beyond the cavity gap, where it has no effect on the measured noise. We are convinced of this because application of a small bias voltage between the cathode and cathode-electrode could change the apparent percentage interception, but  $\Gamma^2$  would remain nearly constant while doing this.

Typical data obtained with these tubes are given in Figs. VI-6 and VI-7. In tube I-4



(VI. TUBE RESEARCH AND DEVELOPMENT)

considerable current was intercepted when the cathode and cathode-electrode were connected together, but making the cathode-electrode a few volts positive with respect to the cathode exerted a focussing effect capable of reducing the interception. In Fig. VI-6 we have plotted  $\Gamma_c^2$  against percent current intercepted, which was varied in this way. Values of  $\Gamma_c^2$  computed from Eqs. (7) and (8) are also plotted, but no interpretations

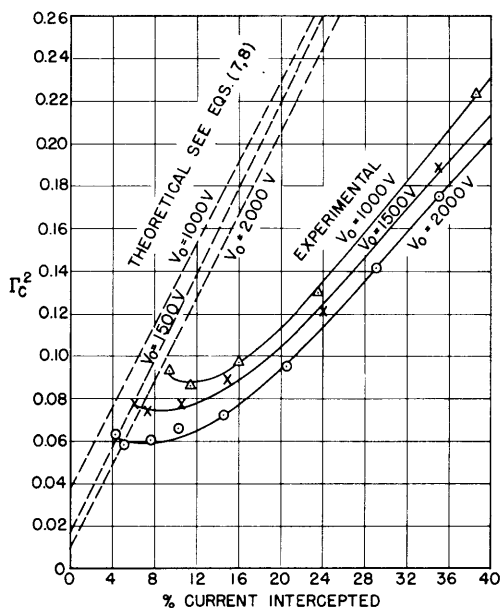


Fig. VI-6 Data on noise factor,  $\Gamma_c^2$ , obtained with tube I-4 at  $T_k = 1105^\circ\text{K}$ .

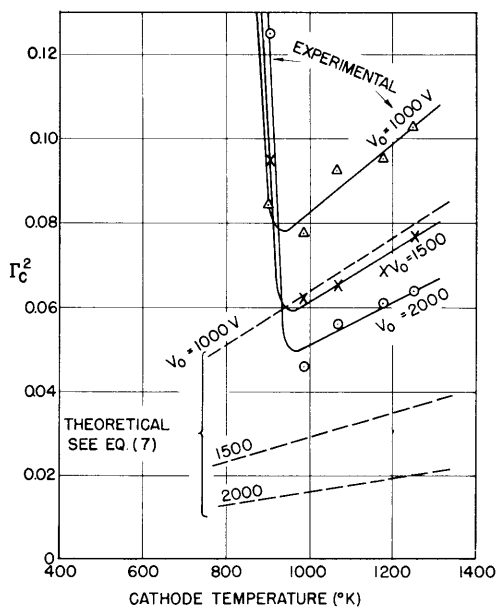


Fig. VI-7 Data on noise factor,  $\Gamma_c^2$ , obtained with tube I-A-6 at zero "bias".

can be made because we do not know just where the stray current is intercepted nor to what extent the bias alters the current distribution in the beam or the transit time. In tube I-A-6, as previously mentioned, we believe  $p_c$  was negligible. In Fig. VI-7 we see that when the cathode temperature is too low to provide adequate emission,  $\Gamma_c^2$  is very high, but as soon as the space-charge-limited condition is established,  $\Gamma_c^2$  is proportional to the absolute cathode temperature, as predicted by Eq. (7). We can also note that  $\Gamma_c^2$  decreases as  $V_0$  increases, which is in qualitative agreement with Eq. (9), but we cannot find quantitative agreement regarding the inverse-square dependence on  $V_0$ .

d. New construction

To check the dependence of  $\Gamma_c^2$  on distance  $x_2$ , a new tube, having a metal bellows to permit changing  $x_2$ , is now nearing completion.

A. Karp

(VI. TUBE RESEARCH AND DEVELOPMENT)

References

- (1) W. W. Mumford: B.S.T.J. 28:4, 608-618 (1949).
- (2) S. C. Brown, D. J. Rose, et al: Technical Reports No. 140 (1949) and No. 66 (1948), Research Laboratory of Electronics, M. I. T.
- (3) A. H. W. Beck: Velocity-Modulated Thermionic Tubes (Cambridge, 1948).
- (4) F. B. Llewellyn: Electron Inertia Effects (Cambridge, 1939).
- (5) F. B. Llewellyn, L. C. Peterson: Proc. I.R.E. 32, 144 (1944).
- (6) L. C. Peterson: Proc. I.R.E. 35, 1264-1272 (1947).
- (7) A. J. Rack: B.S.T.J. 17:4, 592-619 (1938).
- (8) D. O. North: R.C.A. Rev. 5:2 244-260 (1940).

2. Debunching Forces in a Beam of Finite Diameter

In the Llewellyn small signal analysis of the high-frequency behavior of infinite, parallel-plane diodes, the debunching forces in the electron stream take on considerable importance. The application of these equations to beam devices (traveling-wave tube, etc.) has raised some questions as to their direct applicability.

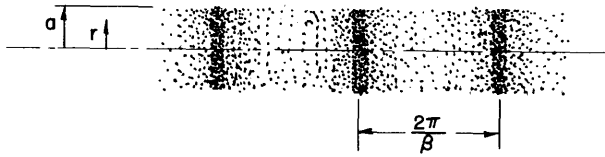


Fig. VI-8 Density modulated beam.

In an effort to get a measure of the reduction of the debunching forces due to the finite beam diameter, the following problem was studied: a stationary, infinitely long beam of electrons, radius  $a$ , and density  $\rho = \rho_0 + \rho \cos \beta z$  (Fig. VI-8). The axial potential due to a thin cylinder

of charge of radius  $r$  and surface density  $\lambda \cos \beta z$  is

$$\phi_1 = A I_0(\beta r) \cos \beta z \quad (r < r_1)$$

and

$$\phi_2 = B K_0(\beta r) \cos \beta z \quad (r > r_1)$$

where

$$A = \frac{K_0(\beta r)}{I_1(\beta r) K_0(\beta r) + I_0(\beta r) K_1(\beta r)} \left( \frac{\lambda}{2\pi \epsilon r} \right)$$

$$B = \frac{I_0(\beta r)}{I_1(\beta r) K_0(\beta r) + I_0(\beta r) K_1(\beta r)} \left( \frac{\lambda}{2\pi \epsilon r} \right)$$

Thus, to get the potential due to a solid beam we must integrate  $\phi_1$  and  $\phi_2$  from  $r_1 = 0$  to  $r_1 = a$ . This operation gives

$$\phi_r = \frac{\rho \cos \beta z}{\epsilon} \left\{ I_0(\beta r) \left[ \beta a K_1(\beta a) - \beta r K_1(\beta r) \right] + K_0(\beta r) \left[ \beta r I_1(\beta r) \right] \right\} = \frac{\rho \cos \beta z}{\epsilon} F$$

(VI. TUBE RESEARCH AND DEVELOPMENT)

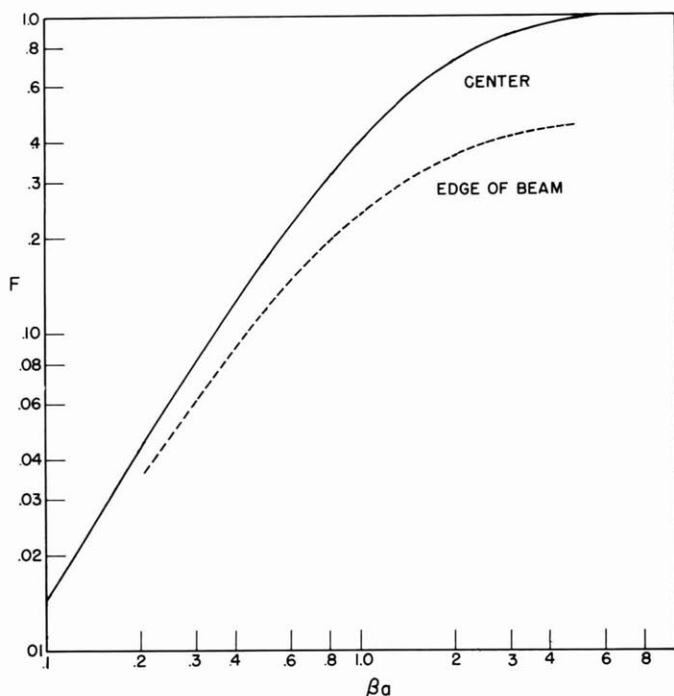


Fig. VI-9 Reduction in debunching force due to finite beam diameter.

The axial field is

$$E_r = -\frac{\partial \phi}{\partial z} = \frac{\beta f \sin \beta z}{\epsilon} (F) \quad .$$

Figure VI-9 is a plot of F for the edge of the beam and the center of the beam, against  $\beta a$ . For  $\beta a \gg 1$ , the value of  $F_{r=0}$  approaches unity, and  $F_{r=a}$  approaches 1/2. Since the field in an infinite parallel plane flow is

$$E = \frac{\beta \rho}{\epsilon} (\sin \beta z) \quad ,$$

F gives the reduction in debunching force due to finite beam diameter. The presence of a conducting drift tube will, of course, reduce F still further.

L. D. Smullin

### 3. Electron Beam Measuring Technique

In the development of electron guns for traveling-wave tubes and other applications it has become necessary to develop a technique for observing the beams produced. The general scheme is shown in Fig. VI-10. A suitable detector screen and collector are mounted on a slug which is free to slide on a tungsten rod within the evacuated tube. This permits observing the beam shape as a function of distance from the anode of the gun. A large coarse screen cylinder is placed around the beam and detector screen to

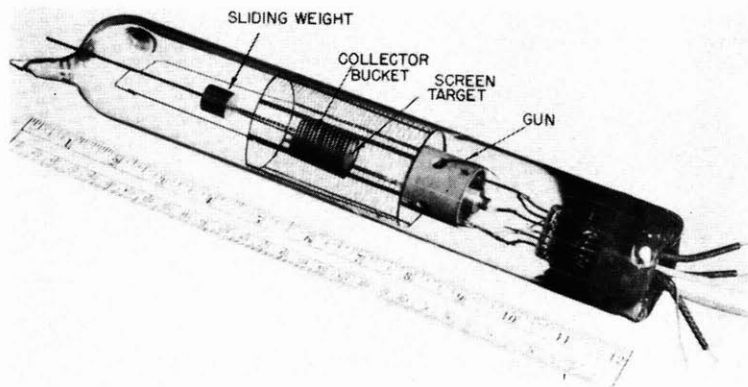


Fig. VI-10

Tube for exploring beam size of 2000 v-5 ma gun.

(VI. TUBE RESEARCH AND DEVELOPMENT)

collect the secondary electrons emitted by the detector screen and collector.

Electron beams with power densities of the order of 30, 800, and 8000 watts/in<sup>2</sup> have been of particular interest. The problem has been one of finding a suitable detector screen material for the different beam power densities.

A willemite coated tantalum disk was used for the low power density beam, but due to the low current saturation of the willemite the relative current distribution over the spot could not be determined. The low electrical conductivity of the willemite resulted in an accumulation of negative charge on the screen. The exact effect of this negative charge upon the beam is unknown.

A screen made of 0.0004-in. thick platinum foil was used for the 800 watts/in<sup>2</sup> beam power density. A visible red spot was produced due to heating of the metal, but the high thermal conductivity of the platinum made the exact beam diameter uncertain. At the higher power density of 8000 watts/in<sup>2</sup> the platinum screen melted.

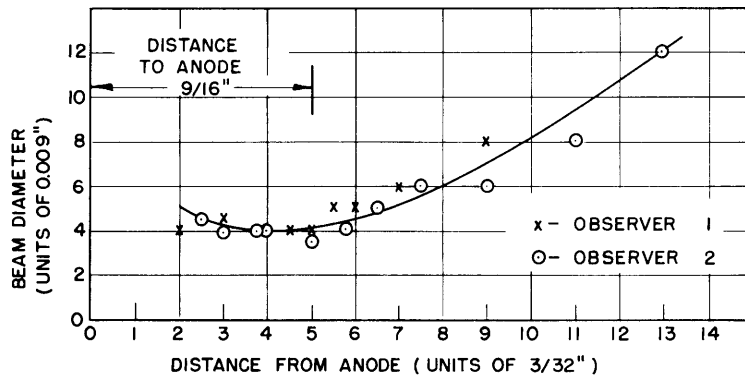


Fig. VI-11

Data obtained using tungsten wire screen with 2000 v-5ma gun.

To try to avoid spot spreading due to heat conduction a screen consisting of 0.0014-in. diam tungsten wire spaced 0.009 in. apart was tried with moderate success. Figure VI-11 shows data obtained by two different observers using this screen, the discrepancies being due to the discontinuous nature of the screen and the vagueness of the spot boundary.

At present a fourth type of screen is being tested. It consists of a very thin coating of graphite on a thoria disk. The high melting points of carbon and thoria and the possibility of obtaining a coating of aquadag thin enough to have a high thermal resistance without too high an electrical resistance makes this screen seem very promising.

G. W. Zeoli

4. Dense Electron Beams in Axial Magnetic Fields

a. Theoretical

Several aspects of this problem have been considered theoretically in the past quarter.

The first of these is the effect of positive ions on the electron beam. Complete space-charge neutralization was assumed since the focussing conditions for this case are easily

## (VI. TUBE RESEARCH AND DEVELOPMENT)

obtained, and because it represents an extreme case. These conditions are prescribed by a certain locus on the design charge described in the last Quarterly Progress Report.

The question of whether such neutralization will indeed take place has also been considered. Although no definite answer has been found, several of the factors involved have been determined qualitatively. Loss of electrons produced by ionization by motion along the beam will, of course, be greater than the similar loss of positive ions. It appears, however, that the positive-ion loss due to transverse motion will be greater than that of the secondary electrons because of the axial magnetic field. A radial sorting effect, too, is present which tends to produce a dipole layer that flattens the potential distribution across the beam.

Some detailed examination of the conditions at the end of the magnetic field has been carried out. It is important to coordinate properly the electron gun, the varying magnetic field, and the potential distribution at the input end of the beam so that the restrictions imposed in the analysis will be actually satisfied. A general treatment of this problem has not been attempted but certain specific methods are proposed.

The magnetic fields of the two focussing solenoids have been calculated. Since the problem is set up in terms of flux linkages (see last Quarterly Progress Report) this calculation is essentially a mutual inductance problem. The calculated and measured values are in excellent agreement.

### b. Experimental

Some of the experimental work on this problem has been started. Both of the focusing solenoids are complete and, as mentioned above, their fields have been measured.

A demountable vacuum system designed to be used in conjunction with a standard laboratory work table has been constructed but not yet tested.

Some parameters of the beam system have been chosen and the electrodes are being fabricated. An electron gun has been designed by means of the electrolytic tank. This gun is now ready for assembly and test.

Considerable time was taken up in developing a suitable heater for the large ring-shaped cathode. The heater power is of the order of 50 watts. The winding is bifilar and is shaped in a flat spiral by hooking it over a pin and winding it into the spiral grooves in the face of a stainless-steel jig. A flat cover facilitates the winding and holds the wire in place while it is being annealed. These heaters have been tested and found suitable for their purpose.

It may be of interest that other types of heaters were formed in which the jig or mandrel had to be dissolved chemically. In every case the heater was warped beyond usefulness. It was finally proved that the chemical treatment alone was responsible for the warping and this method was abandoned.

L. A. Harris

## (VI. TUBE RESEARCH AND DEVELOPMENT)

### C. THE GENERATION OF MILLIMETER AND INFRA-RED RADIATION BY ACCELERATED ELECTRONS

The development of a 20-kv pulsed gun and bunching cavity is in the final stages of completion. The problem of spinning the tantalum electrodes used in the Pierce gun has finally been solved as indicated in the initial tests on the first of the two nearly built tubes. Peak currents of the order of 70 percent of the calculated value have been obtained through a 1-mm-diam iris, 1/4 in. deep, 2 in. from the anode; and of over 98 percent of the calculated value through a 1.5-mm iris.

This current (0.2-0.3 amp) will be more than sufficient for injection into the microwave accelerating cavity which is calculated to drive the electrons up to 1.5 Mev. The first tube and accelerating cavity are being assembled for measuring the electron energy distribution. Following these measurements, the apparatus will be set to generate radiation at 1.25 cm for convenience in detection.

P. D. Coleman